J. Plasma Fusion Res. SERIES, Vol. 3 (2000) 169–175

Plasma Edge Physics and Island Divertor Studies in Wendelstein 7-AS

McCORMICK Kent*, GRIGULL Peter, KÖNIG Ralf, BRAKEL Rudolf, FUCHS Christian, FENG Yuhe, FIEDLER Stefan, GIANNONE Louis, HARTFUSS Hans-Jurgen, HARTMANN Dirk, HILDEBRANDT Dieter, KISSLINGER Johann, KNAUER Jens, KÜHNER Georg, JAENICKE Rolf, NAUJOKS Dirk, SALLANDER Jesper, SARDEI Francesco, WENDLAND Christoph and the W7-AS Team

Max-Planck-Institut für Plasmaphysik, EURATOM Association, Garching, Germany

(Received: 18 January 2000 / Accepted: 17 April 2000)

Abstract

Core, edge and scrape-off-layer (SOL) plasma behavior is studied principally under conditions of an $\iota_a = 5/9$ boundary island configuration, which will be the primary modus operandi for the upcoming W7-AS divertor campaign. Present results are gained with ten inboard sector limiters. High densities, both in the core for central confinement and at the edge for promotion of good divertor operation, are necessary for optimal operation in future steady-state devices. On W7-AS operation at such densities, at low input power $P_{heat} \leq 0.4$ MW, invariably leads to a transition to the ELM-free H-mode, accompanied by low edge densities and augmented core radiation leading to radiation collapse. The threshold density n_e^{thr} necessary to attain the H-mode increases with P_{heat}, such that at $P_{nbi} \sim 2$ MW the H-mode is completely suppressed and peak densities at the separatrix and divertor exceeding 9×10^{19} m^{-3} and 1.5×10^{20} m^{-3}, respectively, are transiently realized. Operation with ECRH at intermediate powers can produce ELMing discharges with the potential of attaining steady-state. The efficacy of newly-installed control coils designed to manipulate the island geometry is tested. Their expected influence on core plasma and boundary-island properties is verified in proof-of-principle experiments. Further technical achievements relevant to future stationary plasma operation on next generation devices are: a) the successful test of a polarimetric diagnostic to measure the line integrated density, based on the Cotton-Mouton effect, and b) demonstration of effective ICRH discharge cleaning in the presence of a magnetic field.

Keywords:

stellarator, W7-AS, divertor, H-mode, density limit, high recycling, plasma-wall-interaction

1. Introduction

An essential feature of any fusion-reactor device, whether tokamak or stellarator, is the capability of plasma-facing components to handle the associated power and particle fluxes, in particular those to divertor target plates. Whereas progress on tokamaks has been substantial, with indications that an ELMy H-mode might qualify as a steady-state solution for both core confinement as well as divertor conditions, investigations on stellarators to this end are in their infancy. The concept of a boundary-island divertor configuration, native to the Wendelstein stellarator research line, has now been tested in a preliminary sense for W7-AS with inboard sector limiters – in preparation for genuine divertor module operation beginning in the summer of 2000. Emphasis has been placed on experimental optimization of both core- and edge-conditions, with a supplementary view towards aspects of steady-state.

*Corresponding author's e-mail: gkm@ipp.mpg.de

W7-AS is a low-shear, 5-period modular stellarator (R = 2 m, $a_{eff} \leq 0.18$ m). Each period contains an "upper" and "lower" inboard sector limiter, making for a total of ten limiters. These limiters are now being replaced by ten divertor modules (with neutral baffling and titanium pumping), optimized for operation with 5/9 islands [1-3]. The 5/9 configuration represents a good compromise between large island size (~ 5–6 cm radially and poloidally) and reasonable effective plasma radius r_{eff} ~ 14 cm, in addition to a favorable geometry in the divertor-target region - thus the motivation for concentration on ι_a ~ 5/9 in these studies.

The boundary islands have the responsibility of isolating the core plasma from the plasma-target interaction region. This can be realized only if perpendicular transport is not so large that it leads to a short-circuiting of the islands, thereby eliminating the gradients along field lines requisite for good divertor action. On the other hand, some perpendicular transport is desireable in order to spread the heat load at the target plates. The contrast between the upstream-downstream connection length L_c (distance between the middle of the island perimeter bordering the LCFS and the target) of ~ 60 m on W7-AS and the island width of ~ 5 cm illustrate the critical dimensions involved. In order to quantitatively influence the balance between parallel-perpendicular transport at constant ι_a, ten control coils have been newly installed. Section 2 reports on initial results.

According to the International Stellarator Scaling [4] energy confinement increases as $\tau_E^{ISS95} \sim n_e^{0.51}$, implying that future ignition devices will necessarily operate in a high density regime. In parallel, high separatrix densities n_{es} are also predicted to be indispensable for efficacious divertor action. In fact, the EMC3 code [5,6] (no impurities) predicts for W7-AS that total detachment will set in when $n_{es} \geq 2 \times 10^{20}$ m^{-3} for 200 kW power to the target plates. In preparation for the divertor phase, efforts have been directed towards documenting edge-limiter plasma behavior at different densities and heating powers, as well as optimizing conditions for the largest possible separatrix density. Section 3 deals with these endeavors. It transpires that the H-mode plays a dominant role in dictating what must be done to enhance n_{es}.

Section 4 summarizes two technical achievements related to steady-state operation of future stellarators.

2. Control Coil Experiments

The influence of the control coils on the plasma was explored in two different approaches. First, since the coils not only can change the size of the islands, but also of the main plasma, the effective plasma radius was varied over the range possible [1]: r_{eff} ~12–16 cm for winding currents I_{cc} = –3.5 to 3 kA (8 windings/coil), ι_a ~ 5/9, P_{nbi}~0.4 MW, n_e~10^{20} m^{-3}. Experimentally, the effect on stored energy W_{dia} was registered, with the result $\tau_E \sim W_{dia} \sim a_{eff}^2$. τ_E^{ISS95} scales as $a_{eff}^{2.2}$, meaning the vacuum field predictions of a_{eff} associated with I_{cc} are in reasonable agreement with those found experimentally via the change in W_{dia}.

The second method was to vary L_c and observe the change in power and particle deposition patterns on the inner limiters. (ι_a ~0.56, P_{ecrh} ~ 0.4 MW, n_e plateaus at 3 & 6 × 10^{19} m^{-3}). The expectation is with shorter L_c that the half-width will become smaller. Fig. 1 illustrates the 2D H_α pattern at this iota. Detailed field-line tracing indicates that the pattern shapes can be entirely dictated by mutual "shadowing" of the limiters; that is, the

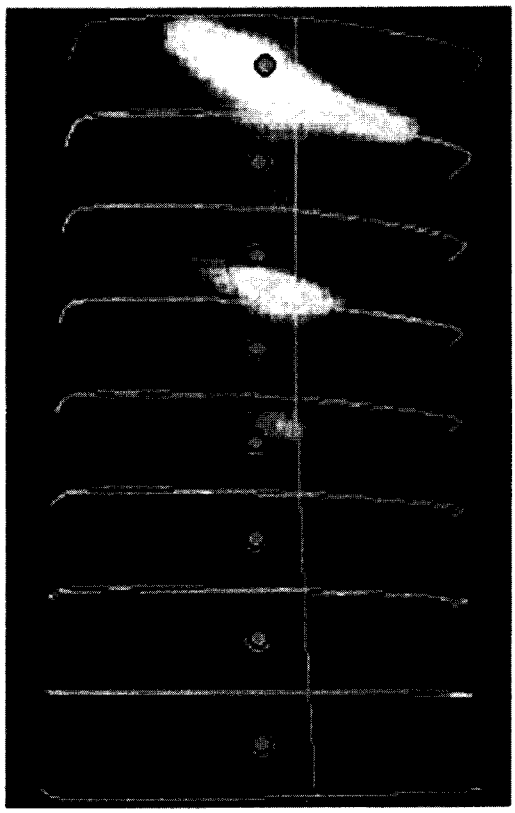

Fig. 1 H_α pattern on inner limiter. Equivalent positions of Langmuir probes are shown for each of the eight tiles. Horizontal x vertical dimensions = 120 × 240 mm. #47129, 0.35sec, P_{nbi} = 2 MW, B_t = 2.5 T, B_z = 86G.

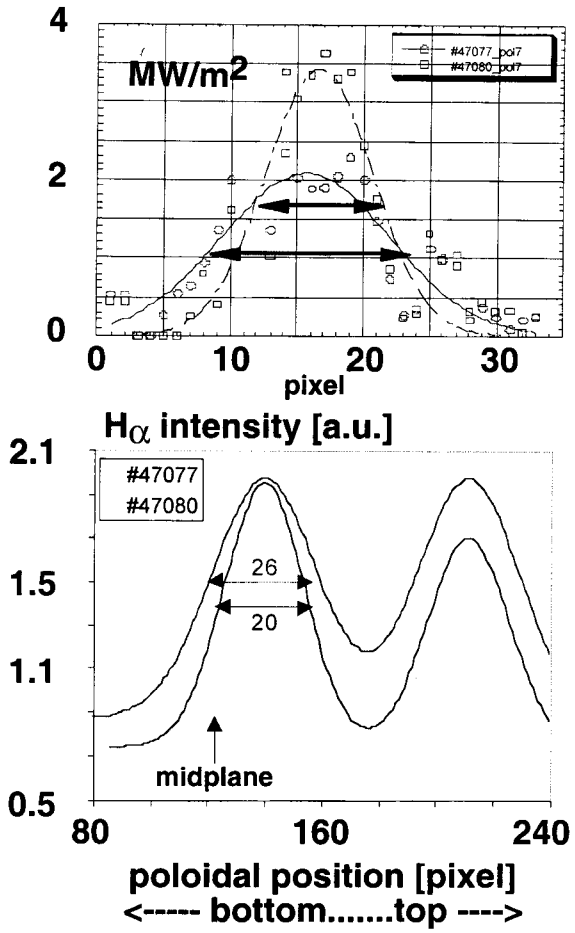

Fig. 2 Power deposition (top) and H_α-profile (bottom) along a poloidal cut across the limiter about in the plane of the Langmuir probes. Only the midplane region is shown. The narrower profiles correspond to shorter L_c (#47080).

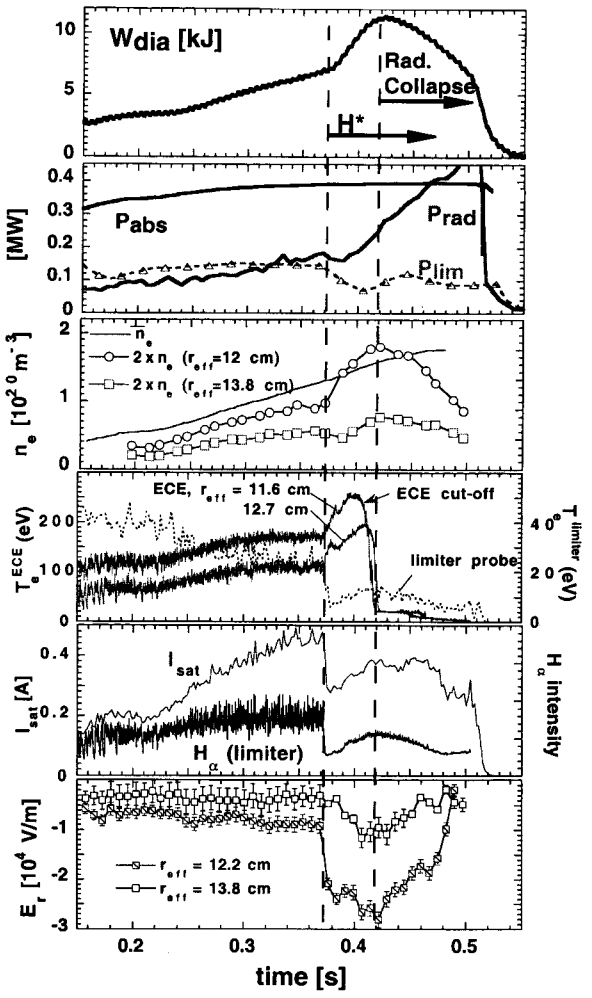

Fig. 3 Temporal evolution of an NBI discharge exhibiting an H* transition. P_{nbi} ~ 0.4 MW (H^0->D^+), B_t = 2.5 T, ι_a ~ 0.558, a_{eff} ~ 14 cm, #45265. Diamagnetic energy W_{dia}, absorbed power P_{abs}, radiated power P_{rad}, power to limiters P_{lim}, edge and line density, edge T_e (from ECE; > 0.4 s cutoff occurs due to increasing n_e) and limiter T_e (Langmuir), saturation current to Langmuir probe, H_α at limiter, radial electric field E_r.

mechanical setup of the limiters with respect to each other creates a spatial filter restricting the deposition area to regions smaller than governed by transport – thereby producing a constancy in profile shape regardless of plasma transport properties [1] (eg. H-mode vs. L-mode, or variation of L_c). The top of the limiter in Fig. 1 exhibits these properties, whereas the limiter middle does not. By changing I_{cc} from 0 to –3.5 kA (larger pitch angle in island-> shorter L_c), L_c for the middle region varied as 110–60 m, respectively. The result is shown in Fig. 2. There is a contraction in the power deposition width of ~ 40%, and in H_α of ~ 25%. Qualitatively, the effect is in the direction expected, indicating we will have some control over the balance between perpendicular and parallel transport in definitive boundary island experiments with the divertor.

3. The H-Mode and Achievement of High Separatrix Densities

Optimum divertor operation (high n_e, low T_e at target) requires attainment of high n_{es} at the lowest possible input power. Density ramp discharges at ι_a~5/9 with P_{nbi}~0.4 MW were found to fall invariably into the ELM-free H-mode H* above a threshold density n_e^{thr}. Fig. 3 depicts the temporal evolution of such an example. At the transition into H*, P_{rad} increases dramatically along with W_{dia}. Transiently, τ_E ~2 τ_E^{ISS95} is reached, but then a radiation collapse begins to set in.

The radial electric field shows the usual rapid increase at the edge normally associated with an H-mode. Other characteristic features at the transition are an increase in n_e and T_e inside the separatrix. This is juxtaposed to the dramatic drop in particle flux to the limiters as documented by the saturation current to a Langmuir probe I_{sat} and H_α, as well as power to the limiters as seen by thermography. The density gradient in the transport barrier region augments particularly spectacularly -changing from $\delta n_e \sim 2 \times 10^{19}$ to $\sim 10^{20}$ m^{-3} over 4 mm (Fig. 4).

The appearance of a new H-mode window around $\iota_a \sim 5/9$ appears to be consistent with a former picture of the necessity of a resonance-free zone in the transport barrier region [7-9]. This may be of relevance to W7-X which exhibits a similar field structure of resonance-free zones for standard configurations. A new aspect is the discovery that n_e^{thr} increases with P_{heat}. As an example, for $\iota_a \sim 0.558$: $n_e^{thr} \sim 0.9\ (P_{nbi} + 1)$ [10^{20} m^{-3}, MW], over $P_{nbi} \sim 0.4$–1.2 MW. Note that the behavior of n_e^{thr} with respect to both n_e and P_{heat} is exactly the opposite to that of tokamaks [10]. On W7-AS one obtains the H-mode by increasing n_e (also seen on COMPASS-D [11]) and decreasing P_{heat}.

Fig. 5 illustrates plasma behavior for different P_{ecrh} (~ 0.4, 0.8 MW) during a density ramp. For 0.4 MW, the discharge drops into the ELM-free mode below 10^{20} m^{-3}. However, at 0.8 MW only "ELMing" activity is evident in H_α for even higher densities. An interesting side effect is that at 0.8 MW the discharge goes through

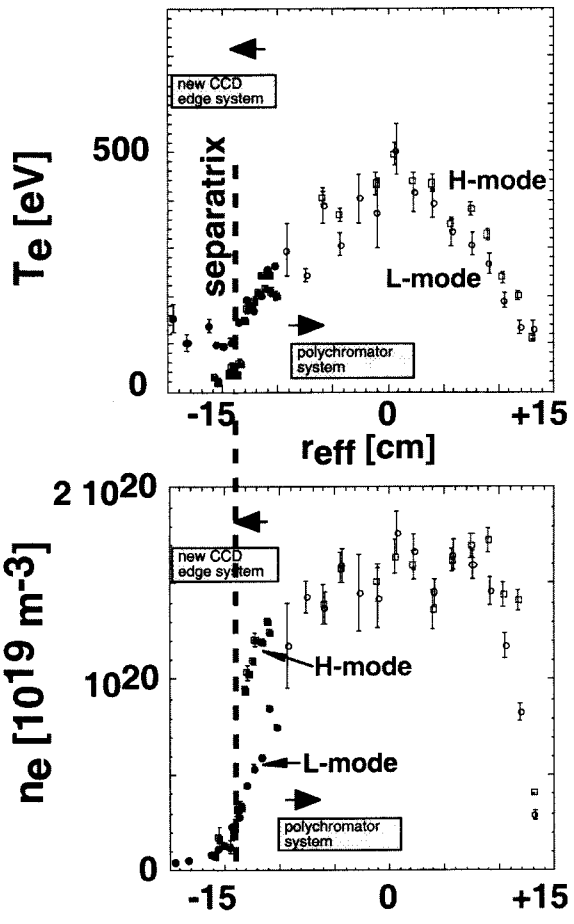

Fig. 4 T_e and n_e-profiles vs. r_{eff} for L- and H*- modes (#48142, 48147 respectively). The new edge-dedicated Thomson system measures to the left of –10 cm. The H*-phase exhibits very steep n_e-profiles just inside the separatrix, with the gradient changing from $\delta n_e \sim 3 \times 10^{19}$ (L-phase) to 10^{20} m^{-3} over 4 mm [17] – the H- and L-mode points are denoted in this region.

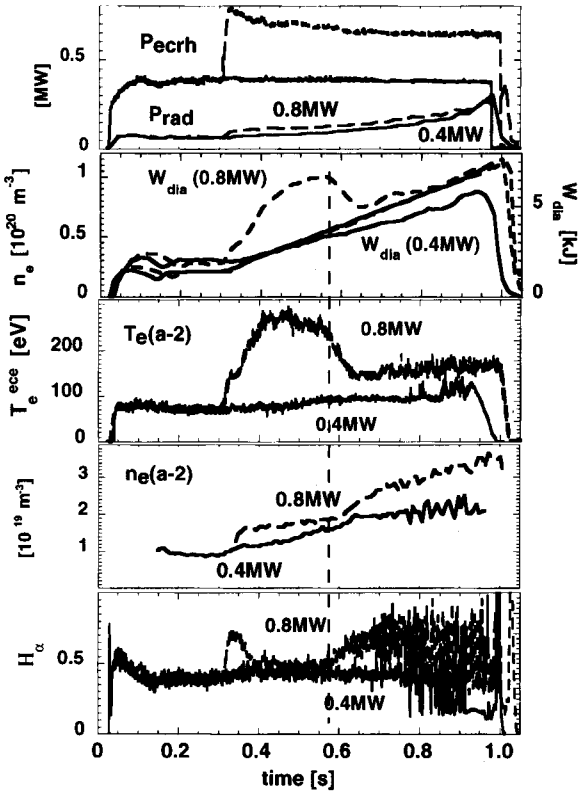

Fig. 5 ECRH power, radiated power P_{rad}, stored energy W_{dia}, line-averaged density n_e, n_e (Li-beam) and $T_e^{ece} \sim 2$ cm inside the separatrix, E_r from BIV spectroscopy, H_α intensity and Langmuir probe densities at an upper inboard limiter. $\iota_a = 0.564$, $B_t = 2.5$ T. Dashed line gives the approximate end of enhanced confinement (for 0.8 MW). #46333, 46337.

a phase of enhanced confinement (compare W_{dia}, T_e(a-2) for 0.4 and 0.8 MW) in the lower density range. Here, the particle (H_α) and power (not shown) fluxes to the limiters are suppressed over this period, as well as n_{es} (not shown). Nonetheless, at higher densities, n_{es} is enhanced at the higher power. The relationships are roughly: $n_{es} \sim 0.083\, n_e + 0.33$ (10^{19} m^{-3}; for $n_e \leq 8 \times 10^{19}$ m^{-3}, 0.4 MW); and $n_{es} \sim 0.15\, n_e + 0.6$ (for 0.8 MW). Due to the ELMing activity, n_{es} often lies below the 0.8 MW characteristic for $n_e > 10^{20}$ m^{-3}.

Whereas n_{es} for these discharges ($n_{es} \sim 2 \times 10^{19}$ m^{-3} for 0.8 MW and $n_e = 10^{20}$ m^{-3}) is far below that predicted essential for good divertor operation, the possibility of using ELMs to avoid core impurity accumulation and an eventual density limit driven by core radiation collapse [12] makes such scenarios potentially attractive. Fig. 6 shows a discharge ($P_{ecrh} \sim$ 0.8 MW, $n_e \sim 10^{20}$ m^{-3}) where over the 0.7s of high power and ELMing activity P_{rad} as well as $Z_{eff}(0)$ appear to be coming into equilibrium.

To maximize the separatrix density it is necessary to completely suppress the H-mode. At $P_{nbi} \sim 2$ MW such is the case. Fig. 7 summarizes the results of two density-ramp discharges with the difference being that the 2nd discharge (#47129) had a still stronger puff – about 20 times higher than the beam fuelling rate. The consequence of the heavy puff is to significantly enhance n_{es} for otherwise the same line density. n_{es} approaching 9×10^{19} m^{-3} is achieved for $n_e \sim 2.5 \times 10^{20}$ m^{-3}. At the limiter n_e exceeds 1.5×10^{20} m^{-3}, with $T_e <$ 10 eV. n_e^{lim} follows the characteristic $\sim n_{es}^2$ (not shown), which is weaker than that expected from the 2-point model ($n_e^{lim} \sim n_{es}^3$). The maximum density actually achieved cannot be determined as the interaction zone shifted away from the Langmuir probe at higher densities (seen by H_α).

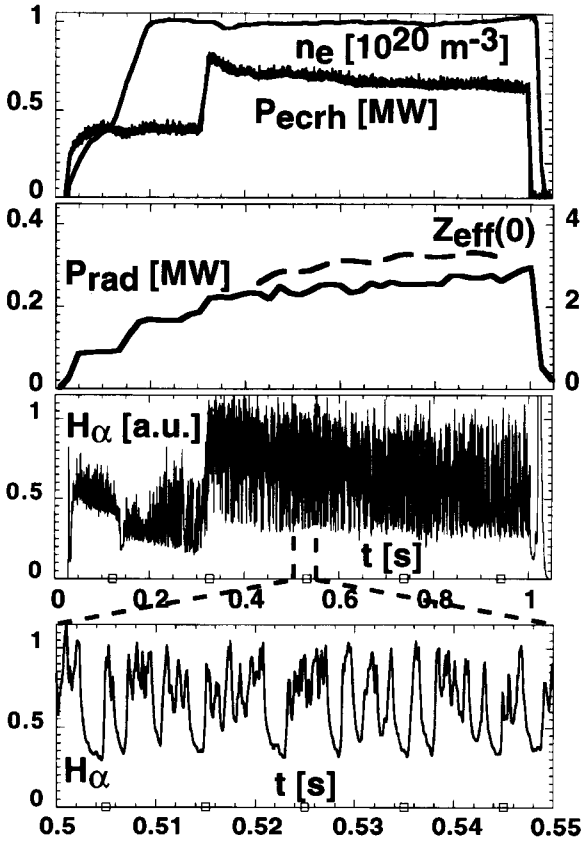

Fig. 6 Density, P_{ecrh}, P_{rad}, $Z_{eff}(0)$, H_α at limiter. Over the discharge, and for 0.5–0.55 sec. #46356

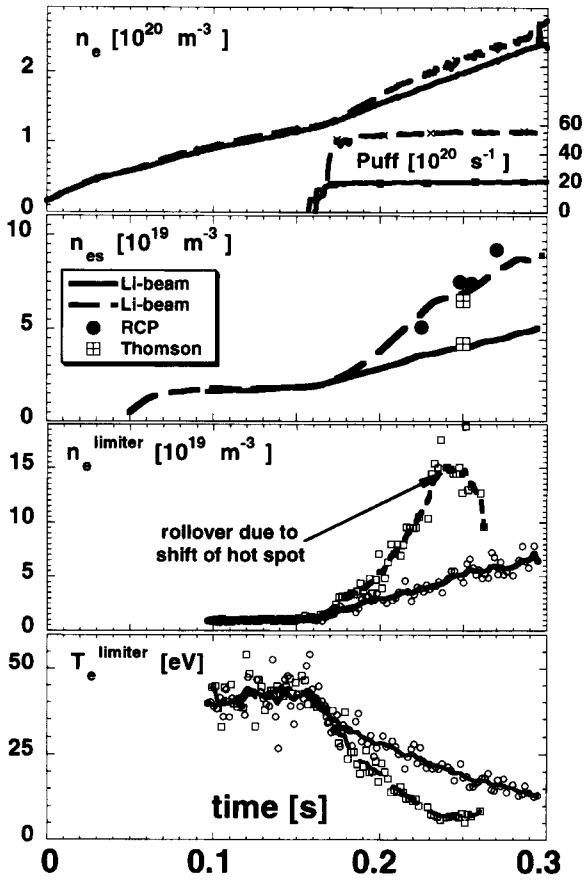

Fig. 7 n_e for two discharges with gas puff as indicated (#47128-full traces, 47129-dashes). n_{es} from Li-beam (traces), RCP (dots) and edge Thomson (squares). n_e and T_e at lower limiter from a Langmuir probe. P_{nbi} = 2 MW, $P_{abs} \sim$ 1.8 MW. Electron fuelling rate from NBI is ~ 2.5 x 10^{20} s^{-1}. H°->D$^+$.

4. Technical Contributions to Stationary Operation

Two technical achievements relating to steady-state machine operation have been realized on W7-AS recently. One is implementation of a polarimetric diagnostic measuring the line integrated density based on the linear birefringence of the magnetized plasma, called the Cotton-Mouton effect. The other has to do with ICRH discharge cleaning in the presence of a magnetic field.

An overriding requirement for density control of stationary discharges is the availability of an absolute and robust measurement of the integrated line density. A single-channel polarimeter based on the Cotton-Mouton effect and operating in the submillimeter wave region of 500–650 GHz has demonstrated proof-of-principle on W7-AS [13,14]. Even at densities in the 10^{20} m^{-3} range the phase shift remains below 360°, thereby eliminating the need to keep track of fringe shifts. The magnetic field geometry of W7-X offers similarly good properties as those of W7-AS in terms of diagnostic demands (*e.g.* constant B-field along the line of sight), so this technique is destined to become of primary importance in long-shot phases of W7-X.

Conventional glow discharge cleaning (GDC) techniques do not function with a magnetic field. However, the advent of superconducting field coils in future experiments such as W7-X necessitates that ways be found to effect wall conditioning under such circumstances. To this end, ICRF-assisted wall conditioning experiments have already been carried out on the tokamaks TEXTOR and Tore Supra. Initial efforts on W7-AS have lead to positive results [15]: Due to the confining field afforded by a stellarator, plasmas of reasonable density ($\leq 2.5 \times 10^{18}$ m^{-3}) and temperature (edge T_e up to 30 eV) can be maintained, leading to a wall desorption of hydrogen comparable to that attained with GDC. Results are insensitive to magnetic field strength (0.3 T, steady-state or 1.25 T, 5-sec pulse). An important preliminary finding is, in contrast to tokamak experience, that hydrogen desorption seems to increase with power density P_{ICRF}/p_{He} (P_{ICRF} up to 120 kW, p_{He} = He pressure).

5. Discussion

The predicted influence of newly-installed control coils on the core plasma radius and on the balance between perpendicular and parallel transport in boundary islands has been qualitatively verified. Thus, we may expect the coils to become a useful tool in more definitive experiments performed under divertor conditions. – particularly so as the edge diagnostic set is being greatly expanded [16].

The appearance of a new H-mode window around $\iota_a \sim 5/9$ seems compatible with previous theoretical considerations regarding the absence of lower-order resonances in the transport barrier region in order to avoid viscous damping of E × B poloidal rotation [7-9]. Within this window it is found that the threshold density n_e^{thr} for entering the H-mode increases with power [9]. This behavior is opposite that of tokamaks where one crosses the threshold by lowering density or raising the power, and not vice versa. A new edge Thomson scattering system in its run-in phase has documented extremely high density gradients inside the separatrix during the ELM-free H-mode [17]. Overall, more definitive H-mode insights on a broader basis must await the upcoming operational period.

In order to enhance confinement or the edge density, it is necessary to increase n_e. At low P_{heat} (~ 0.4 MW) and for $\iota_a \sim 5/9$ (relevant for divertor operation), discharges invariably fall into the ELM-free H-mode with ensuing low n_{es} and rapidly increasing core radiation, generally ending in radiation collapse. Higher powers facilitate "ELMing" discharges, which might have steady-state significance in terms of avoiding the density limit associated with radiation collapse. At 2 MW the H-mode is suppressed on W7-AS. Global density profiles also broaden, thereby augmenting the separatrix density. n_{es} of around 9×10^{19} at $n_e \sim 2.5 \times 10^{20}$ m^{-3} has been attained in heavy-puff, transient, density-ramp discharges – whereby n_e at the limiter exceeded 1.5×10^{20} m^{-3}, with $T_e < 10$ eV. Edge behavior with the new divertor modules may be expected to be different owing to the somwhat larger neutral penetration lengths from the target plates to the core plasma as compared to the inner limiters, as well as to the greatly improved neutral baffling. In any case, we should be in good position to provide an edge-target database against which the EMC3 code can be benchmarked. This will be the primary contribution to W7-X, aside from establishing values for size scalings between W7-AS and W7-X. We note, the more favorable boundary island geometry on W7-X [18] should promote, for example, easier entry into the detached regime than on W7-AS, so many W7-AS findings will not find direct application to W7-X

Work on installation of the divertor modules is proceeding as planned, with expected start-up in the summer of 2000. Figure 8 shows one set of the modules

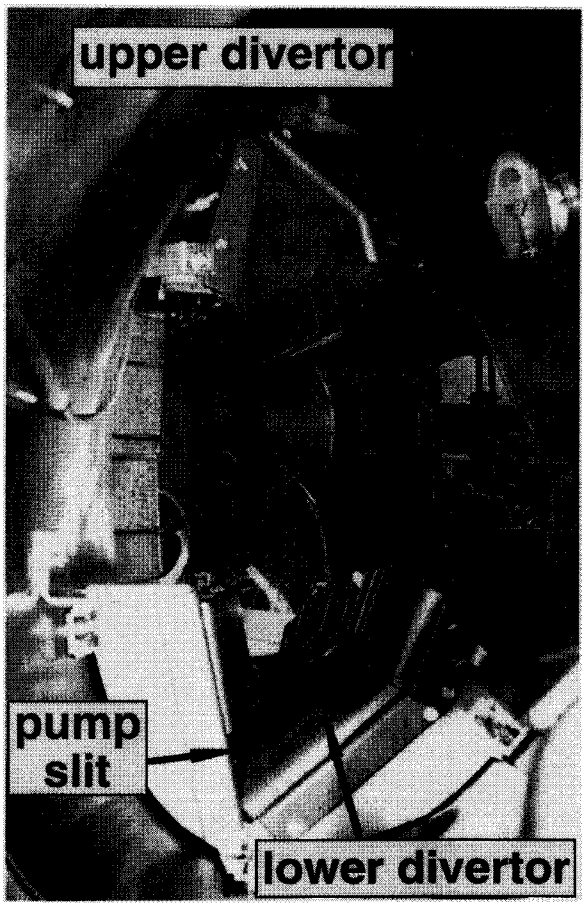

Fig. 8 View of one up-down divertor module pair in W7-AS.

already mounted. Almost all of the plasma-wall interaction will be at the target plates, instead of only about 50% as in the case of the inner limiters. This should allow higher heating levels for longer times. With NBI 3 MW can be injected for 3 sec from 8 PINIs. The four 140 GHz gyrotrons (cutoff $n_e = 1.2 \times 10^{20}\,m^{-3}$) will deliver 2.2 MW(1s) or 1 MW(2s) or 0.6 MW(3s).

References

[1] K. McCormick, P. Grigull *et al.*, Plasma Phys. Contr. Fusion **41**, B285–B304 (Dec. 1999).

[2] P. Grigull *et al.*, J. Nucl. Mater. **241-243**, 935 (1997).

[3] F. Sardei, Y. Feng, P. Grigull *et al.*, J. Nucl. Mater. **241-243**, 135 (1997).

[4] U. Stroth, M. Murakami, R.A. Dory, H. Yamada, S. Okamura, F. Sano and T. Obiki, Nucl. Fusion **36**, 1063 (1996).

[5] Y. Feng, F. Sardei, J. Kisslinger and P. Grigull, J. Nucl. Mater. **241-243**, 930 (1997).

[6] Y. Feng, J. Kisslinger and F. Sardei, 26th EPS Conf. (Maastricht), Europhysics Conf. Abs. **23J**, 1465 (1999).

[7] H. Wobig and J. Kisslinger, Proc. 24th EPS Conf. Vol. 4, 1669 (Berchtesgaden, 1997).

[8] H. Wobig and J. Kisslinger, private communication.

[9] P. Grigull, M. Hirsch, K. McCormick *et al.*, 26th EPS Conf. (Maastricht), Europhysics Conf. Abs. **23J**, 1473 (1999).

[10] W. Suttrop *et al.*, Plasma Phys. Control. Fusion **39** (1997) 2051

[11] S.J. Fielding, *et al.*, 7th IAEA Meeting H-mode Meeting (Oxford, 1999) to appear in Plasma Phys. Contr. Fusion.

[12] L. Giannone, *et al.*, these proceedings.

[13] C. Fuchs and H.J. Hartfuss, Phys. Rev. Lett. **81**, 1626 (1998).

[14] C. Fuchs and H.J. Hartfuss, Rev. Sci. Instrum. **70**, 722 (1999).

[15] R. Brakel, 14th PSI meeting (Rosenheim, 2000).

[16] K. McCormick *et al.*, Proc. 12th Int. Stellarator Conf. (Madison, 1999).

[17] J.P. Knauer *et al.*, Proc. 12th Int. Stellarator Conf. (Madison, 1999).

[18] J. Kißlinger, IPP Report 2/331, 148 (Jan. 1996).